Dynamic System Simulation with Hybrid Thermal Storage Tanks

Sarah Jäger*, Peter Renze

Institute for Technology and Energy Economics, University of Applied Sciences Ulm, 89075 Ulm, Germany,
*sarah.jaeger@thu.de

SNE 36(2), 2026, 65-71, DOI: 10.11128/sne.36.tn.10771
Sel. ASIM GMMS/STS 2025 Postconf. Publication: 2025-10-22
Received Extended: 2026-01-30; Accepted: 2026-02-15
SNE - Simulation Notes Europe, ARGESIM Publisher Vienna
ISSN Print 2305-9974, Online 2306-0271, www.sne-journal.org

This paper is focused on recent advancements in the integration of thermal storage systems with phase change material (PCM) packed beds for energy storage applications. A simulation environment is presented that combines detailed PCM modeling with dynamic load profiles corresponding to specific consumers and producers. By incorporating individual building and user parameters, this approach provides the foundation for simulating and analyzing application scenarios and their impact on the thermal performance of storage systems with different PCM configurations, compared to a conventional stratified water tank.

Introduction

The model is based on a one-dimensional mathematical approach that represents temperature distributions in two zones (Jäger et al. 2024). It is adaptable to arbitrary tank geometries and various PCM layer configurations and is currently being enhanced to investigate storage behavior under dynamic operating conditions.

The thermal dynamics within the water zone of the storage tank during charging or discharging processes are modeled as an open system with energy and mass exchange.

This is described through differential equations for discrete tank, accounting for heat loss to the environment, conduction between layers using an effective conductivity, mass flow during charging and discharging processes, and heat transfer between water and PCM capsules.

1 Modelling

The governing equations describe the temporal evolution of thermal energy within discretized storage layers. For a generic layer i, where $i = 1, \dots, n$, A_{ax} denotes the base area of the cylindrical control volume. The formulation for the bottom layer of the water zone is given by:

$$\begin{aligned}\rho\, c_p\, A_{ax}\, \varepsilon\, \Delta z \frac{dT_1}{dt} &= A_{Tank}\, U_{Tank}(T_{amb} - T_1) + \\ &+ \frac{\lambda_{eff}\,(A_{ax} - \varepsilon)}{\Delta z}\,(T_2 - T_1) + \\ &+ \dot{m}_{down}\, c_p\, (T_2 - T_1) + \\ &+ \dot{m}_{up}\, c_p\, (T_{dis} - T_1) + U_C\, A_C\, (T_{PCM1} - T_1)\end{aligned} \tag{1}$$

For the intermediate layers between the bottom and top of the storage tank:

$$\begin{aligned}\rho\, c_p\, A_{ax}\, \varepsilon\, \Delta z \frac{dT_i}{dt} &= A_{Tank}\, U_{Tank}\, (T_{amb} - T_i) + \\ &+ \frac{\lambda_{eff}\,(A_{ax} - \varepsilon)}{\Delta z}(T_{i-1} - 2\,T_i + T_{i+1}) + \\ &+ \dot{m}_{down}\, c_p\, (T_{i+1} - T_i) + \\ &+ \dot{m}_{up}\, c_p\, (T_{i-1} - T_i) + U_C\, A_C\, (T_{PCM\,i} - T_i)\end{aligned} \tag{2}$$

For the last layer *n* at the tank top:

$$\begin{aligned}\rho\, c_p\, A_{ax}\, \varepsilon\, \Delta z \frac{dT_n}{dt} &= A_{Tank}\, U_{Tank}\, (T_{amb} - T_n) + \\ &+ \frac{\lambda_{eff}\,(A_{ax} - \varepsilon)}{\Delta z}\,(T_{n-1} - T_n) + \\ &+ \dot{m}_{down}\, c_p\, (T_{ch} - T_n) + \\ &+ \dot{m}_{up}\, c_p\, (T_{n\text{-}1} - T_n) + U_C\, A_C\, (T_{PCM\,n} - T_n)\end{aligned} \tag{3}$$

Heat exchange with the environment is represented by a wall heat transfer term, whose coefficient U_{Tank} depends on internal and external flow conditions as well as on the thermal properties of the tank wall and insulation and may vary along the tank height.

For the bottom and top layers, the effective tank area additionally includes the corresponding end surfaces, which generally leads to increased thermal interaction compared to intermediate layers. Axial heat transport between adjacent layers is represented by an effective thermal conductivity that accounts for heat conduction through both the water domain and the tank wall, thereby capturing the additional vertical heat flux induced by the high thermal conductivity of the metallic storage wall and its influence on thermal mixing (Untrau et al. 2022).

The PCM domain is modelled by a separate energy balance (4), assuming heat exchange exclusively with the surrounding water and no interaction with adjacent layers. Heat transfer between the water and the PCM capsules, as well as heat conduction within the capsules, is represented by a temperature-dependent overall heat transfer coefficient U_C, while phase change is modeled using an enthalpy-based approach.

$$\rho\, c_p\, A_{ax}\,(1-\varepsilon)\,\Delta z\,\frac{dT_i}{dt} = U_C\, A_C\,(T_i - T_{PCM\,i}) \qquad (4)$$

Zones within the tank are determined based on PCM placement and inlet and outlet locations, and if no PCM is present, the corresponding heat transfer term is omitted. As the PCM capsules form a packed-bed configuration within the storage tank, only a portion of the total tank volume is available for the water phase.

This portion is described by the porosity ε, which is defined as the ratio of the void volume to the overall tank volume. The void volume is obtained by subtracting the total volume of the PCM capsules from the tank volume, yielding

$$\varepsilon = \frac{V_T - V_{PCM}}{V_T} \qquad (5)$$

A schematic representation visualizing the described model is provided in Figure 1.

2 Experiments and Results

Developed in MATLAB, the model was validated using experimental data from a hardware in the loop test facility, successfully simulating continuous charging scenarios. This integration of simulation and experimental validation enables a comprehensive evaluation of storage system performance under realistic conditions.

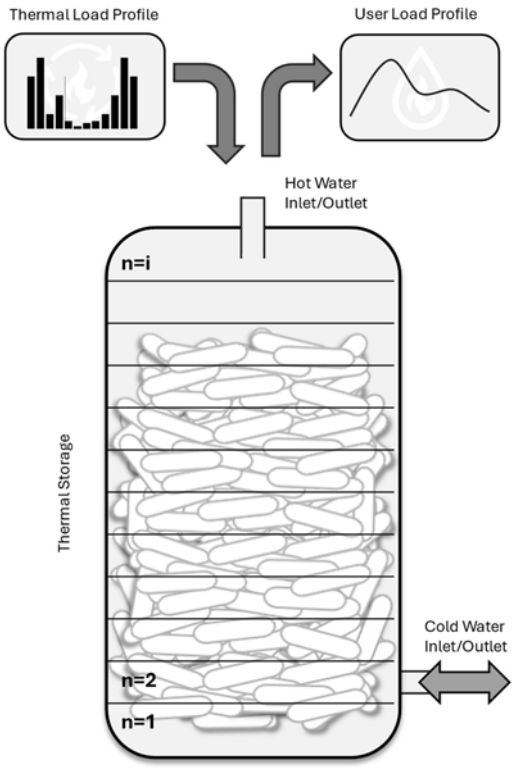

Figure 1: Schematic representation of the hybrid thermal storage model, illustrating the surrounding system modeled as load profiles.

The recent modifications enabling predefined charging and discharging profiles to be implemented by converting hourly energy demands of both consumers and heat generators, defined at specified hot water temperature levels, into corresponding volume flow rates entering or leaving the tank, thus directly affecting the energy balance calculations of the discretized tank layers.

A domestic hot water tank with $V = 2$ m³ was top loaded at $\vartheta = 60$ °C and discharged following a standard family load profile (Bundesverband Wärmepumpe (BWP) e.V. 2023).

The study compared three tank configurations without losses: an ideal stratified tank, a tank filled with PCM capsules with a melting point of 58 °C, and one with capsules at 37 °C.

A 24-hour segment of a simulation cycle is presented in Figure 2. The first column illustrates the hourly temperature distribution along the tank height, while the second column depicts the stored heat distributions at each 2 cm layer of height. The PCM58 capsules did not fully melt in this scenario.

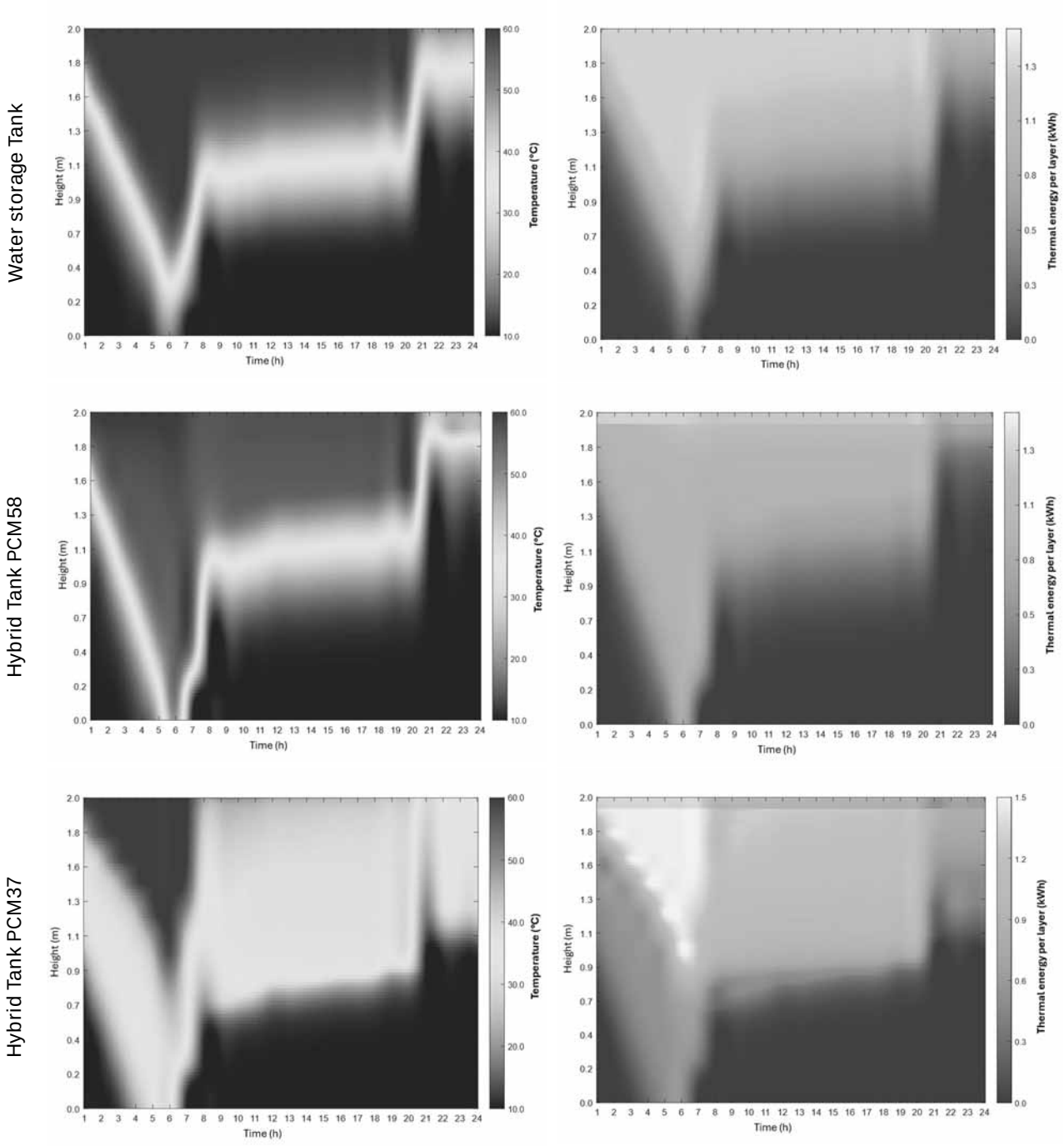

Figure 2: Temperature Distribution and Stored Heat for each of 100 Layers across a 24-Hour Segment of a Simulation

In contrast, the PCM37 configuration demonstrated a higher energy density spreading downward until hour 6, indicating significant latent heat absorption.

Despite storing 109 kWh (PCM37) at its peak or immediately after the last charging hour, compared to 83.5 kWh (PCM58), the temperature in the upper_section of the PCM37 tank decreased more rapidly during discharge, reaching 38 °C by hour 21.

At the same time, the PCM58 tank retained 52 °C, while the stratified tank provided 57 °C. After discharge (after hour 22), both PCM tanks exhibited slight reheating, stabilizing near the melting temperature of the respective PCM.

For this scenario, the stratified tank maintained a stable hot water temperature over a longer time period, proving to be the better option when a minimum temperature of 55 °C is required.

For this scenario, the stratified tank maintained a stable hot water temperature for a longer period when a minimum temperature of 55 °C is required.

To place this observation into a broader context, the following section examines the applied control strategy and the temporal availability of energy above the usable temperature level. Comparable boundary conditions are ensured through a temperature-based control approach. The system temperature is limited to a usable level of 55 °C, which corresponds to the required supply temperature of the building.

Charging of the storage tank is controlled by a simple temperature based controller that stops charging once an upper temperature limit is reached in defined storage regions. This prevents the storage tank from being fully heated, particularly in the lower section. After a defined hysteresis, charging is enabled again. During discharge, heat supply to the consumer is stopped if the temperature falls below 55°C.

For comparison, the storage systems are simulated over extended periods under identical conditions with respect to storage volume, control strategy, charging logic, load profile and temperature requirements on the consumer side. The weekday load profile differs slightly from the weekend profile, with higher domestic hot water demand occurring later in the day on weekends. Differences between the systems therefore result only from the use of PCM capsules and the associated increase in energy density at the melting temperature.

Figure 3 illustrates the evaluation approach, showing the total stored energy relative to a reference temperature of 10 °C as a solid gray line, while the fraction of energy above the usable temperature level of 55 °C is indicated by a dashed gray line.

For the water storage, charging and discharging occur without restrictions on the usable temperature range. During charging, the temperature in the lower storage region increases gradually until charging is interrupted by the controller.

As a result, the water storage is able to supply the consumer continuously over the entire simulation period.

The hybrid storage using PCM with a melting temperature around 58 °C can store more energy at the desired temperature level, although this energy cannot always be delivered immediately. At high discharge rates, temporary temperature drops occur, followed by a temperature recovery. These effects are observed around 22 h on a daily basis. This behavior is caused by the delayed phase change process.

The available sensible heat in the water is utilized. Cool water enters the region of freezing PCM capsules and absorbs latent heat, reheating the water to a slightly higher temperature.

Consistent with this effect, the gray dashed line shows that part of the stored energy remains available at the desired temperature level at the end of the day.

In contrast, the storage system with PCM 37 cannot provide the required supply temperature, even though the total stored energy is higher, since the control strategy allows charging to continue to lower temperature levels before charging is stopped. Toward the end of each day, the temperature drops well below the minimum required level. Although some energy above 55 °C is available at the beginning of each cycle, it is almost completely depleted during the first heat extraction. The PCM latent energy does not contribute, since phase change occurs below the usable temperature level.

Under the investigated boundary conditions, no direct benefit for the consumer is observed from PCM integration compared to an ideal stratified water storage. Although the hybrid tank with PCM and a melting temperature of 58 °C maintains a slightly larger amount of energy at the required temperature level, this additional energy is not accessed in the considered scenario.

This outcome highlights that a higher overall storage capacity alone does not lead to improved consumer level performance and motivates the analysis of alternative load profiles. Advantages arise when the limited discharge power of the PCM capsules is explicitly taken into account. If the maximum discharge power is reduced while the daily energy demand is increased, the PCM storage with a melting temperature of 58 °C provides benefits compared to the water storage.

Under a modified load profile with reduced peak discharge rates within one hour and a higher daily total heat demand, the PCM storage is able to fully cover the demand, as shown in Figure 4.

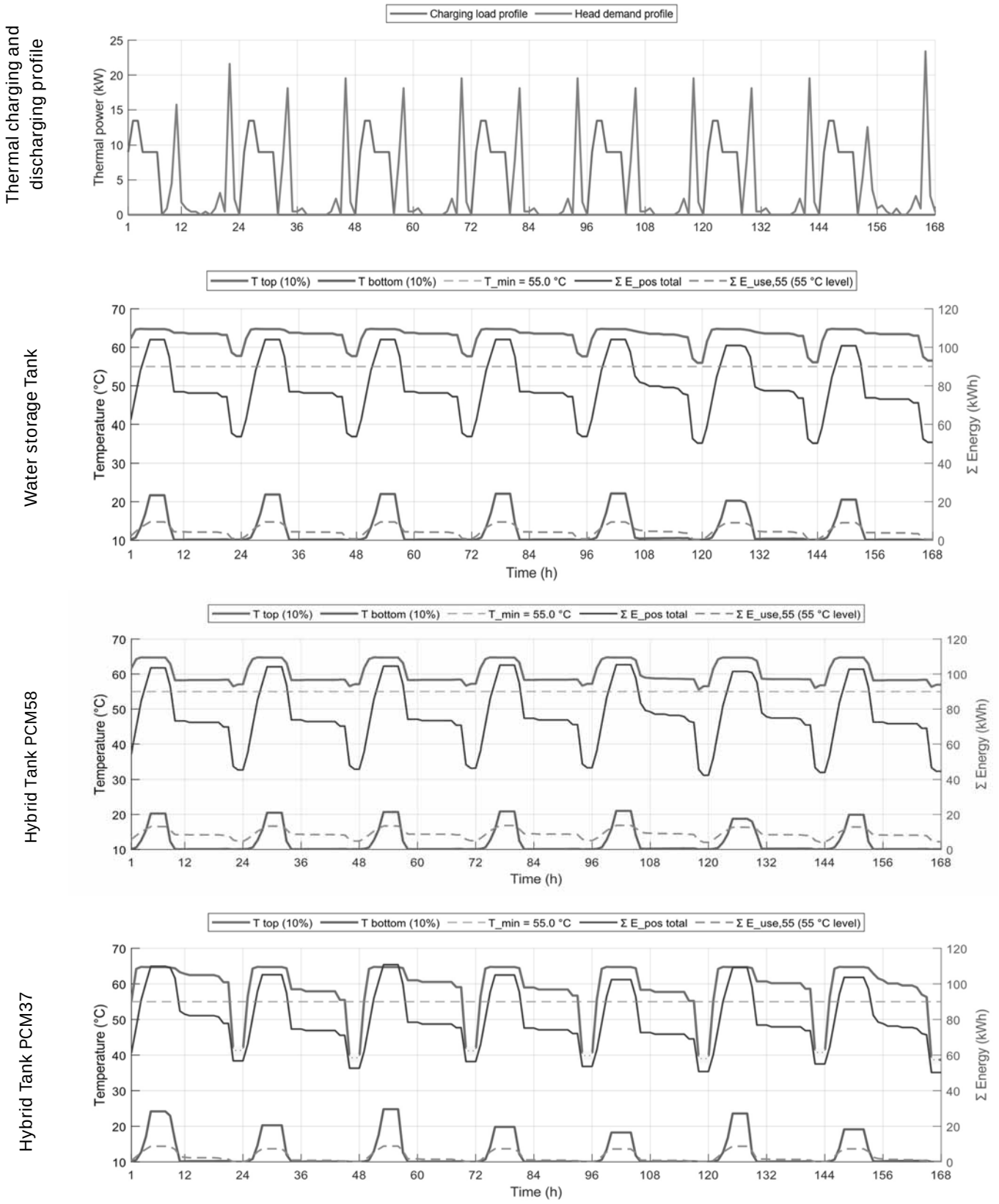

Figure 3: Storage temperatures at the top and bottom and energy level over time under the weekly load profile, including the fraction of energy available above 55 °C.

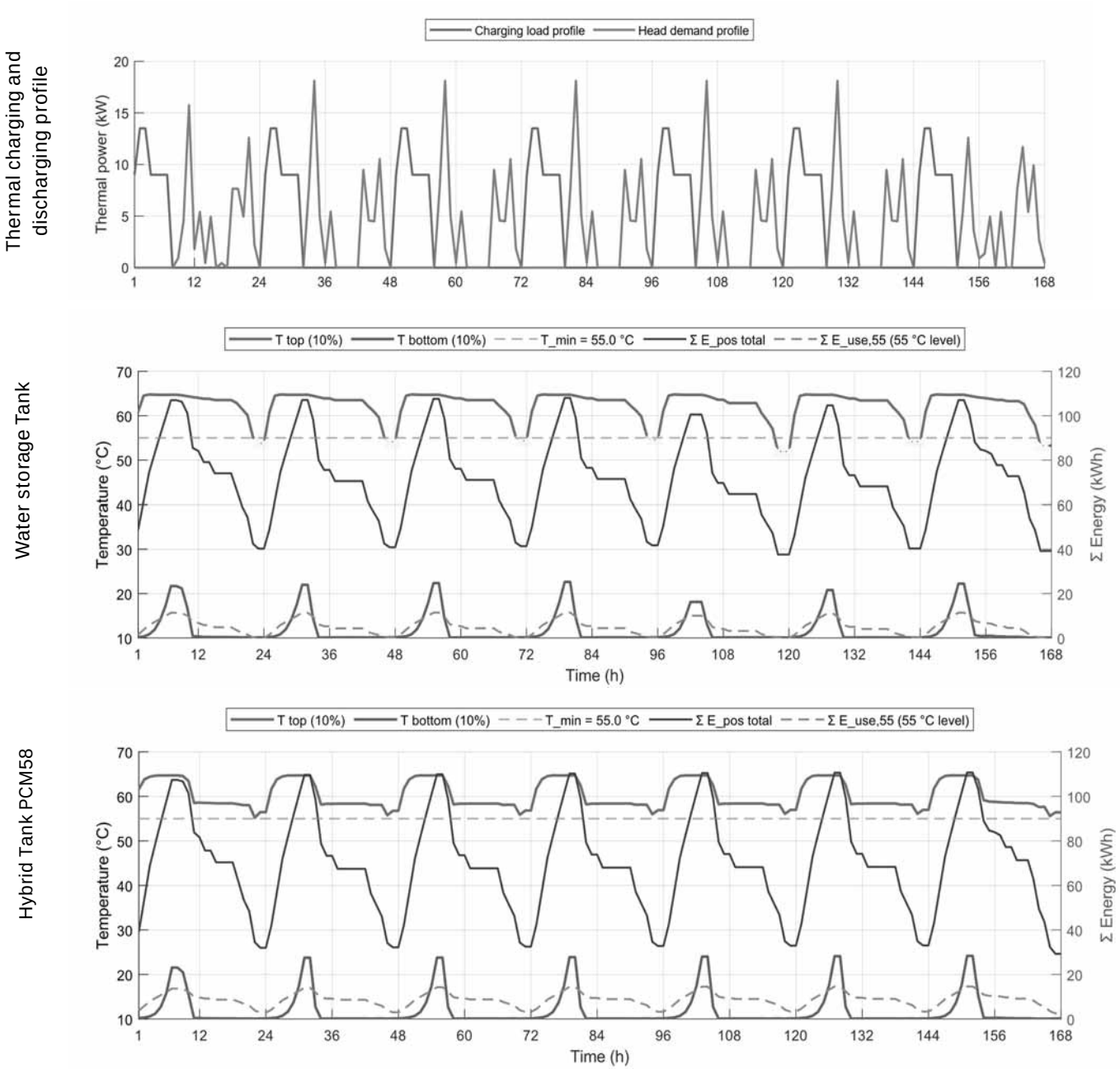

Figure 4: Storage temperatures at the top and bottom and energy level over time under the modified weekly load profile, including the fraction of energy available above 55 °C.

Under the same conditions, the stratified water storage reaches a coverage of 87 percent, leaving 948 hours uncovered out of a total of 7776 hours with heat demand. These results demonstrate that PCM based storage systems can provide benefits under specific operating conditions. In this case, for load profiles with lower peak demands, PCM enables a higher amount of energy to be available at the required temperature level than water storage, while the discharge power remains constrained by the PCM properties and its interaction with the surrounding water.

Further evaluation is required for storage systems with indirect heat transfer and for concepts with multiple charging sources operating at different temperature levels. On the system level, temperature dependent effects must also be taken into account, since both the efficiency of heat generators such as heat pumps and the requirements of consumers strongly depend on the operating temperature level and influence overall system performance.

In addition, long term thermal storage concepts that operate beyond hourly fluctuations should be analyzed to assess their impact on overall system efficiency. Within this context, the presented approach provides a practical tool for evaluating PCM integrated storage systems under dynamic operating conditions.

Nomenclature

Latin Symbols

Symbol	Unit	Quantity
A	m^2	Area
c_p	$J / (kg\,K)$	specific heat capacity at constant pressure
T	K	temperature
t	s	time
U	$W/(m^2\,K)$	overall heat transfer coefficient
V	m^3	volume

Greek Symbols

Symbol	Unit	Quantity
ε	-	porosity
λ	$W/(mK)$	thermal conductivity
ρ	kg/m^3	density

References

[1] Jäger, Sarah; Pabst, Valerie; Renze, Peter (2024): Multizone Modeling for Hybrid Thermal Energy Storage. In: *Energies* 17 (12), S. 2854. DOI: 10.3390/en17122854

[2] Untrau, Alix; Sochard, Sabine; Marias, Frédéric; Reneaume, Jean-Michel; Le Roux, Galo A. C.; Serra, Sylvain (2023): *A fast and accurate 1-dimensional model for dynamic simulation and optimization of a stratified thermal energy storage*. In: *Applied Energy* 333, DOI: 10.1016/j.apenergy.2022.120614

[3] Bundesverband Wärmepumpe (BWP) e.V. (2023): Leitfaden Trinkwassererwärmung. Hg. v. BWP. Online verfügbar unter https://www.waermepumpe.de/verband/publikationen/fachpublikationen/, zuletzt geprüft am 29.01.2025

Publication Remark

This contribution is the significantly extended version of the Workshop proceedings version for

ASIM Workshop GMMS/ STS 2025 - Munich/Oberpfaffenhofen 2025,

published in

ASIM Workshop GMMS/STS 2025 Tagungsband ARGESIM Report 48, e-ISBN 978-3-903347-66-3, Volume DOI 10.11128/arep.48, p 61-63.